DRAFT VERSION MAY 11, 2014
Preprint typeset using LaTeX style emulateapj v. 2/19/04

NON-RADIAL OSCILLATIONS IN M-GIANT SEMI-REGULAR VARIABLES: STELLAR MODELS AND *KEPLER* OBSERVATIONS

DENNIS STELLO,[1,2] DOUGLAS L. COMPTON,[1] TIMOTHY R. BEDDING,[1,2] JØRGEN CHRISTENSEN-DALSGAARD,[2,3] LASZLO L. KISS,[4,1,5] HANS KJELDSEN,[2] BEAU BELLAMY,[1] RAFAEL A. GARCÍA,[6] SAVITA MATHUR,[7]

Draft version May 11, 2014

ABSTRACT

The success of asteroseismology relies heavily on our ability to identify the frequency patterns of stellar oscillation modes. For stars like the Sun this is relatively easy because the mode frequencies follow a regular pattern described by a well-founded asymptotic relation. When a solar like star evolves off the main sequence and onto the red giant branch its structure changes dramatically resulting in changes in the frequency pattern of the modes. We follow the evolution of the adiabatic frequency pattern from the main sequence to near the tip of the red giant branch for a series of models. We find a significant departure from the asymptotic relation for the non-radial modes near the red giant branch tip, resulting in a triplet frequency pattern. To support our investigation we analyze almost four years of *Kepler* data of the most luminous stars in the field (late K and early M type) and find that their frequency spectra indeed show a triplet pattern dominated by dipole modes even for the most luminous stars in our sample. Our identification explains previous results from ground-based observations reporting fine structure in the Petersen diagram and sub ridges in the period-luminosity diagram. Finally, we find 'new ridges' of non-radial modes with frequencies below the fundamental mode in our model calculations, and we speculate they are related to f modes.

Subject headings: stars: fundamental parameters — stars: oscillations — stars: interiors

1. INTRODUCTION

At the beginning of this century, the semi-regular variables were probably the least understood of all variable stars (Wood 2000). In the decade following, we have seen tremendous progress in the study of these stars driven by long-duration ground-based surveys such as MACHO (Wood et al. 1999; Fraser et al. 2005; Riebel et al. 2010), OGLE (Kiss & Bedding 2003; Soszynski et al. 2004; Groenewegen 2004; Ita et al. 2004a; Soszynski et al. 2007), EROS (Spano et al. 2011), and even 'backyard observations' (Tabur et al. 2010). With four years of continuous data from *Kepler*, it has now become possible to investigate the frequency spectra of late K and early M giants using space-based data (Bányai et al. 2013; Mosser et al. 2013).

Semi-regular variables bridge the gap between the lower luminosity G and K giants oscillating in multiple radial and non-radial modes like the Sun (Chaplin & Miglio 2013; Hekker 2013; Mosser 2013; Garcia & Stello 2014), and the radial fundamental-mode 'Mira' oscillators (Olivier & Wood 2005). Key uncertainties concerning semi-regular variables include the transition between so-called 'solar-like' to the much higher amplitude 'Mira-like' oscillations (Christensen-Dalsgaard et al. 2001; Bedding et al. 2005; Xiong & Deng 2013). This includes the question of non-radial modes, which are definitely present in less luminous giants but absent in Miras. There has been a long discussion on the origin, and ultimately the mode orders, associated with the main ridges seen in the period-luminosity diagram for these giants (e.g. Wood & Sebo 1996; Wood et al. 1999; Bedding & Zijlstra 1998; Kiss & Bedding 2003; Ita et al. 2004b; Tabur et al. 2010; Dziembowski & Soszyński 2010; Soszyński & Wood 2013; Soszyński et al. 2013; Takayama et al. 2013; Mosser et al. 2013). Throughout this discussion, it has frequently been assumed that the oscillations in semi-regular variables consist mainly or entirely of radial modes (e.g. Wood et al. 1999; Dziembowski et al. 2001; Soszyński et al. 2013). It was suggested by Dziembowski et al. (2001) and Christensen-Dalsgaard (2004) that strong radiative damping through the coupling to the g modes in the core would make the non-radial modes unobservable. However, using OGLE data Soszynski et al. (2004) noticed features in the so-called Petersen diagram of period ratios that they could not explain purely by radial modes. Soszynski et al. (2007) refined this result, showing fine structure in the Petersen diagram that they suggested could be due to non-radial modes. In an attempt to match model frequencies to the OGLE data, Dziembowski & Soszyński (2010) calculated both radial and dipole mode frequencies but found significant discrepancies between models and observations. In addition to a series of radial modes, Takayama et al. (2013) derived frequencies of a dipole and also a quadrupole mode to explain the fine structure in the Petersen diagram observed by Soszynski et al. (2007). With the shorter but much higher photometric quality *Kepler* data, Mosser et al. (2013) clearly detected non-radial modes among the least luminous stars in their sample. However, they found that the power of the dipole modes decreased dramatically for luminous stars having dominant oscillation frequencies below $\nu_{\rm max} \sim 1\,\mu$Hz (period $\gtrsim 10$ days). During this transition the power of the radial modes increased. Clear evidence for non-radial modes in high-luminosity (M-type) red giants has not been established.

In this Letter we examine the oscillations in late K and early

[1] Sydney Institute for Astronomy (SIfA), School of Physics, University of Sydney, NSW 2006, Australia
[2] Stellar Astrophysics Centre, Department of Physics and Astronomy, Aarhus University, Ny Munkegade 120, DK-8000 Aarhus C, Denmark
[3] Kavli Institute for Theoretical Physics, University of California, Santa Barbara, CA 93106, USA
[4] Konkoly Observatory, Research Centre for Astronomy and Earth Sciences, Hungarian Academy of Sciences, Budapest, Hungary
[5] ELTE Gothard-Lendület Research Group, Szombathely, Hungary
[6] Laboratoire AIM, CEA/DSM-CNRS, Université Paris 7 Diderot, IRFU/SAp, Centre de Saclay, 91191, Gif-sur-Yvette, France
[7] Space Science Institute, 4750 Walnut street Suite 205, Boulder, CO 80301, USA

M giants using both theoretical adiabatic frequency calculations of full non-truncated stellar models and four-year *Kepler* data of about two hundred stars. We show that these stars oscillate in both radial and non-radial modes but with frequency spectra that differ markedly from those of less luminous giants. These differences explain the fine structure seen in the Petersen diagram. Most remarkably, we show that the frequency spectra of M giants are actually dominated by dipole ($l = 1$) modes.

2. THEORETICAL MODELS AND ADIABATIC FREQUENCIES

Calculating frequencies of non-radial oscillations in luminous giants is challenging and computationally intensive because they are mixed modes that arise from coupling between p modes in the envelope and a large number of extremely high-order g modes in the core. Previously, the presence of the core and the coupling with the g modes were neglected (e.g. Dziembowski & Soszyński 2010) or dealt with using a non-adiabatic asymptotic treatment (Dziembowski 2012). Our frequency calculations are based on non-truncated models and take the coupling between envelope and core fully into account. This minimizes the risk of inducing sudden artificial frequency shifts from truncation and hence allows us to follow the oscillation modes from the main sequence to the red giant branch with a self consistent set of model calculations. We calculated adiabatic frequencies using an updated version of ADIPLS (Christensen-Dalsgaard 2008a,; Christensen-Dalsgaard et al., in preparation). To represent the high-order g-dominated mixed modes in the core, the spatial mesh was distributed according to the asymptotic behavior of the eigenfunctions, and the scan for eigenfrequencies was similarly based on the asymptotic distribution. For the most evolved models the g-mode behavior was inadequately resolved by the spatial mesh, even at the highest number of points (around 76,000); however, we have ascertained that this had insignificant effect on the properties of the acoustically dominated modes that we are concerned with here. Our stellar models are derived using the MESA `1M_pre_ms_to_wd` test suite case (Paxton et al. 2011, 2013). We cross-checked our results using ASTEC models (Christensen-Dalsgaard 2008b) and frequencies derived using GYRE (Townsend & Teitler 2013) and found no significant difference to the MESA-ADIPLS results presented here.

Figure 1 shows model frequencies for an evolving star of $1M_{\odot}$. Each symbol represents a mode of degree $l = 0$ (radial), $l = 1$ (dipole), or $l = 2$ (quadrupole). The symbol sizes are scaled by $1/\sqrt{\mathrm{Inertia}_{\mathrm{mode}}}$, normalized to the radial modes, and resemble a frequency-dependent 'pseudo' amplitude (Aerts et al. 2008). To guide the eye, we have connected radial modes of the same order from one model to the next by dotted black lines. We show all frequencies from about 0.1 to 0.9 times the acoustic cut-off frequency. Assuming the oscillations are solar-like, the modes between the two dashed lines are the strongest and most likely to be observed.

Between the dashed lines, the main-sequence models show a pattern closely resembling the asymptotic relation (Tassoul 1980), with dipole modes about halfway between each closely spaced quadrupole-radial pair. When the model reaches the subgiant phase, the core contraction causes the frequencies of the g modes in the core to increase while envelope expansion leads to a decrease of the p-mode frequencies, eventually resulting in an overlap of the two sets of modes (Christensen-Dalsgaard et al. 1995). This leads to coupling of the non-radial modes, resulting in mixed modes whose frequencies can become strongly bumped from the regular p-mode pattern seen during the main-sequence. The effect first becomes visible for the quadrupole modes (Stello 2012), quickly followed by the dipole modes, which show the strongest mode bumping (Figure 1, models with $\nu_{\max} \lesssim 1500\,\mu$Hz).

As the model evolves up the red giant branch the core keeps contracting, resulting in an increase in the density of g modes and in the width of the evanescent zone separating the g- and p-mode cavities. This gives rise to many more mixed modes and a weaker coupling than in the subgiant phase, and we start to see clusters of $l = 1$ mixed modes at each p-mode order ($30 \lesssim \nu_{\max}/\mu\mathrm{Hz} \lesssim 500$) (Dupret et al. 2009; Bedding et al. 2010). This is because several g modes in the core are coupling to each p mode in the envelope. The largest symbols within each cluster reveal the location of the resonant p mode and allow us to follow the evolution of the spacing between this mode and its nearest radial mode along the red giant branch. As pointed out by Bedding et al. (2010), the dipole modes have moved slightly to the right of centre relative to the radial modes (see also Mosser et al. 2011; Huber et al. 2011; Corsaro et al. 2012), a result that was also seen in a series of stellar models by Montalbán et al. (2010). In Figure 1 we see that the dipole modes move even further to the right for more luminous models, eventually forming the left fork of a 'triplet', with the quadrupole mode in the middle and the radial mode to the right (see inset).

The change in the frequency pattern from the main sequence to the luminous giants is due to two factors. Firstly, the excitation shifts to lower-order modes ($\nu_{\max}$ decreases), away from the asymptotic regime. Secondly, we see a change in the frequency pattern at fixed radial order. For example, the positions of the dipole modes (red dotted line) clearly shift relative to that of the radial $n = 5$ ridge.

The change in frequency pattern is further illustrated in Figure 2 with échelle diagrams for the four models marked by arrows in Figure 1. The main-sequence model (Figure 2(a)) shows dipole modes roughly halfway between the radial modes essentially all the way down to the lowest-order modes. The next example (Figure 2(b)) shows an intermediate pattern, where the highest frequency dipole modes are also about halfway between the radial modes, but at lower frequencies they shift closer to the quadrupole-radial pair, resulting in triplet structures. Finally, the very luminous models (Figures 2(c) and (d)) show triplet structures for the entire range.

Another interesting feature in Figure 1 is the presence of non-radial modes with frequencies below the fundamental radial mode. They have low inertia to be visible in Figure 1. These may be related to the 'f modes' found by Cowling (1941) to be intermediate between the g and p modes, in calculations neglecting the perturbation to the gravitational potential (the so-called Cowling approximation). Such modes, with no node in the radial direction, are also found in the Cowling approximation for realistic unevolved models, with frequencies below the fundamental radial mode and inertias only slightly higher than that mode. When the Cowling approximation is not made there is no such f mode for $l = 1$, since with no radial node it would displace the center of mass; however, the f mode with $l = 2$ is still found. A similar mode confined to the envelope could account for the potentially visible $l = 2$ mode below the fundamental radial mode. For the corresponding $l = 1$ mode found in the calculations, largely trapped in the envelope, we speculate that it is similar to the f mode in the Cowling approximation but with a

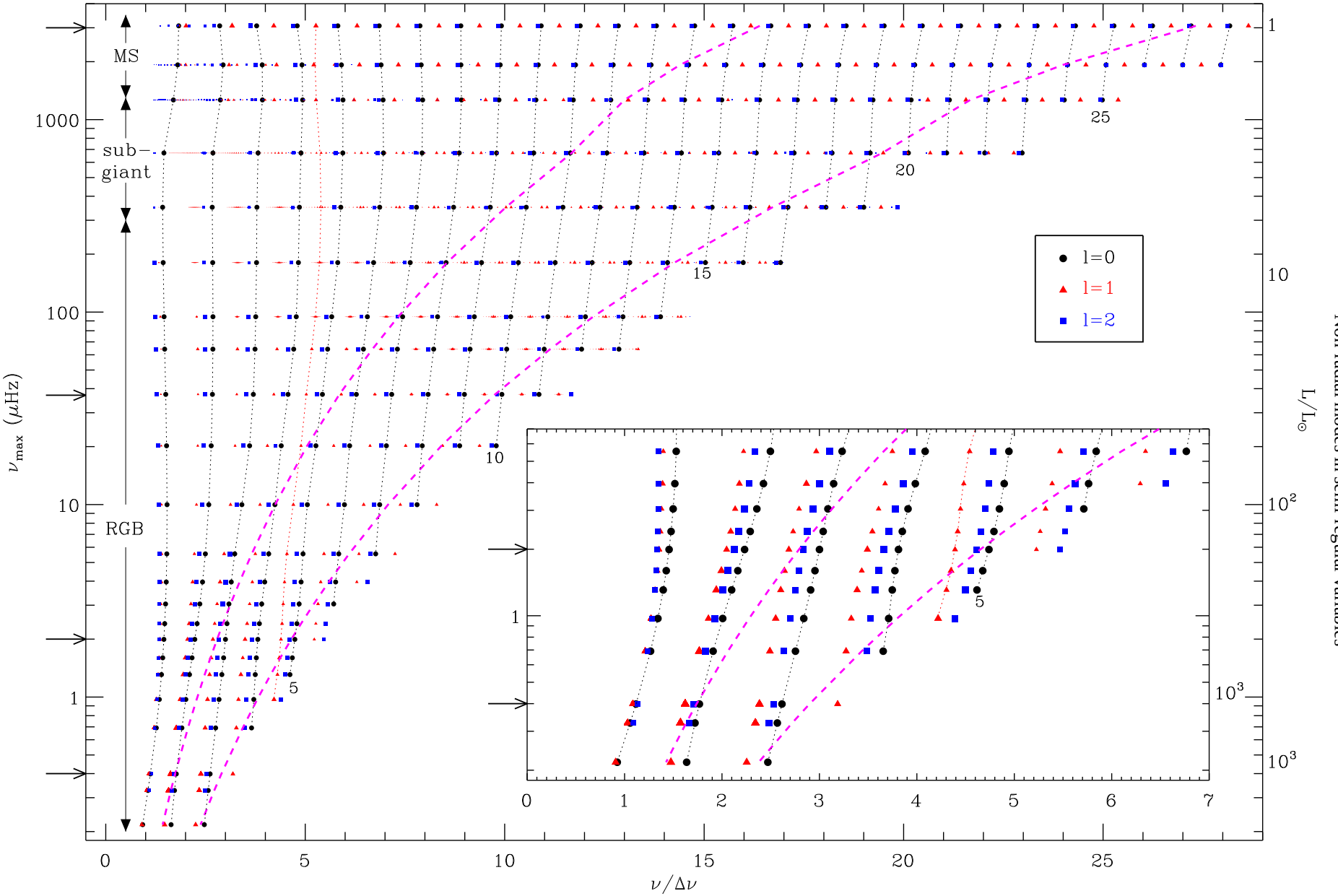

FIG. 1.— Model frequencies, in units of the asymptotic large frequency separation, for solar-metallicity models along a $1M_\odot$ track. Each model is plotted according to its $\nu_{\rm max}$. Symbols for different spherical degrees are indicated to the right, and evolutionary states are indicated to the left. Dotted vertical lines connect radial (black) and dipole (red) modes of the same p-mode order, the former annotated for every $5^{\rm th}$ order. Dashed magenta lines show locations of 75% and 125% of $\nu_{\rm max}$. Horizontal arrows mark models shown in Figure 2. The inset shows a close-up of the lower-left region.

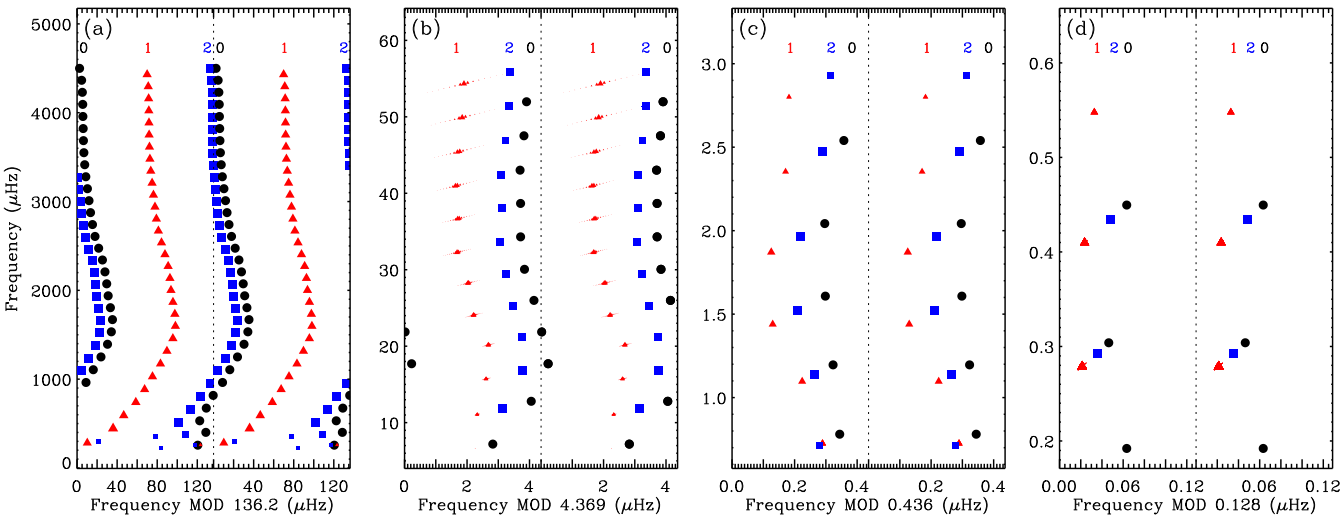

FIG. 2.— Échelle diagrams for four representative models from the main sequence to near the tip of the red giant branch. Mode degrees are indicated for each ridge, and symbol size is scaled as in Figure 1. Each échelle is plotted twice, as indicated by the vertical dotted line.

structure in the core ensuring that the center of mass is not displaced. This calls for further investigation. We speculate that these modes might be related to the extra sequence F in the period-luminosity diagram near the fundamental sequence C (Soszyński & Wood 2013).

3. OBSERVATIONS

We investigated the oscillation spectra of 195 giants that were pre-selected as M-giant targets for the *Kepler Mission*, based on their variability in the ground-based ASAS survey (Pigulski et al. 2009)[8]. The *Kepler* data were obtained between 2009 June 20 and 2013 April 4, corresponding to observing quarters 2 to 16, using the spacecraft's long-cadence mode ($\Delta t \simeq 29.4$ minutes). To correct quarterly flux discontinuities in the data we first grouped stars into 'fast' and 'slow' oscillators based on the number of intercepts of the time series relative to a linear fit to the data using only the first quarter (Q2). We chose 15 crossings as the discriminator, corresponding to a dominate oscillation period of about 11 days. For the 'fast' group we subtracted a linear fit from each quarter and then shifted their mean flux levels to that of the first quarter. For the 'slow' group we made linear fits to the five points on either side of quarterly gaps and shifted the flux to make the two fits intersect at the middle of the gap. Again, we used the first quarter as anchor point for the flux level. However, where the gap was longer than 10 days, we applied the same method as for the 'fast' oscillators.

We ordered the stars by $\nu_{\rm max}$ and stacked their frequency-scaled power spectra, as shown in Figure 3(a). We see clear triplet ridges for each radial order. To construct Figure 3(a) we used the following two-stage approach. First, we examined each spectrum in an attempt to determine a reference frequency, $\nu_{\rm ref}$, of a clearly identifiable mode. For this stage, the reference mode did not need to be the same for all stars. To aid the identification we looked for the strongest modes, assuming they were the ones closest to $\nu_{\rm max}$, and compared with the frequency pattern and $\nu_{\rm max}$ from stellar models (Figure 1). This allowed us to associate the correct radial order with each observed triplet structure for about 40% of the stars. For each remaining star we made an initial guess of the reference mode identification and frequency. We then created a template spectrum as the average of the 10 already-identified spectra with reference frequencies closest to that of the initial guess for the target star. A comparison revealed the correct order of the reference mode for the target star.

With the modes identified for all stars, we then sought to associate values of $\nu_{\rm ref} \equiv \nu_{n=3,l=0}$, $\nu_{\rm max}$, and $\Delta\nu$ for each star based on matching with a grid of models. The main purpose of this second step was to align the spectra relative to a common reference mode and to sort the stars by $\nu_{\rm max}$ with minimal effect from observational uncertainty. The initial matching model, and hence the initial $\nu_{\rm max}$, was found by interpolating the models that bracketed the observed reference frequency found in the previous step. The final best-matching model was found by first generating 50 additional interpolated models that sampled the $\pm 20\,\%$ range around the initial $\nu_{\rm max}$. From these models we then created model spectra, where each mode was represented by a Lorentzian profile with a width equal to the inverse observing time, and mode heights were modulated by a Gaussian envelope centered on $\nu_{\rm max}$ with $\mathrm{FWHM} = 0.25\,\nu_{\rm max}$. By correlating the observed and modelled spectra, we identified the final best model as the one with the strongest correlation. The resulting $\nu_{\rm max}$ was used to sort the stars in Figure 3(a) and $\nu_{\rm ref}$ was used to scale the frequency axis. Each spectrum is represented by a horizontal band with the level of power indicated by the grayscale. The power was normalized for each spectrum by its highest peak. The low-frequency noise was suppressed by multiplying the spectrum by a Gaussian envelope of FWHM = $\nu_{\rm max}$ centered at $\nu_{\rm max}$. For the less-evolved stars, we applied extra smoothing of the spectra proportional to $\nu_{\rm ref}$ in order to produce a common width of the mode ridges. It is quite remarkable how closely the observations follow the model frequencies (solid lines in the background) in this very non-asymptotic regime. This agrees well with the trend seen among K giants, which shows a decreasing offset between the observed and modelled frequencies towards more luminous stars (White et al. 2011).

In Figure 3(b) we show the collapsed version of panel (a). This demonstrates clearly that the dipole modes are generally much stronger than the radial modes, unlike in less evolved stars (see also Mosser et al. 2013 and references therein). It is particularly interesting to note that the dipole modes dominate even for the most evolved stars in our sample (periods ~ 50 days), which seems to go against previous interpretations of semi-regular variables (e.g. Wood & Sebo 1996; Wood et al. 1999; Soszynski et al. 2007). We further note that the triplet structure disappears for the lowest order modes, where we see only a single peak per order. This could be because the ridges of different degrees merge, as suggested by the models, which we cannot adequately resolve with the length of the current data set.

Finally, in Figure 4 we show a representative selection of power spectra for five stars. Based on the above mode identification we indicate the most significant non-radial modes and the first seven radial modes (the fundamental plus the $1^{\rm st}-6^{\rm th}$ overtones) from the best-fitting model found by the interpolation of our stellar model grid. A striking feature in some of these spectra is the frequency pattern forming triplets.

4. THE PERIOD-LUMINOSITY AND PETERSEN DIAGRAMS

Previous analyses of frequencies of semi-regular variables have been based on the period-luminosity diagram and also on the Petersen diagram of period ratios. To allow comparison with previous work on such stars, we show in Figure 5 the period-luminosity diagram of the models shown in Figure 1 (inset) and Figure 3.

The frequency pattern created by the non-radial modes seen in Figures 1 and 2 explains the fine structure in the Petersen diagram seen as sets of closely-spaced horizontal triplet bands (e.g. Takayama et al. 2013), referred to as sub-ridges in the period-luminosity diagram by Soszynski et al. (2007). The highest period ratio of ~ 0.98 mentioned by Takayama et al. (their Figure 7) would emerge from the ratio of two peaks in the power spectrum separated by the frequency resolution of their data set ($1/T_{\rm obs}$), thus associated with the same mode and presumably arising due to stochastic excitation of damped modes, as in less luminous giants. Assuming the excitation is solar-like, we expect all the radial and non-radial modes are excited within a 'broad' envelope centered around $\nu_{\rm max}$. Due to geometrical cancellation, however, we only see modes of degree $l \leqslant 2$ (Figure 3), whose period ratios form the remaining triplet structures.

5. CONCLUSIONS

Our results clearly show the presence of both radial and non-radial modes in semi-regular variables. We demonstrated

[8] Our data were selected as part of the KASC Working Group 12 activities.

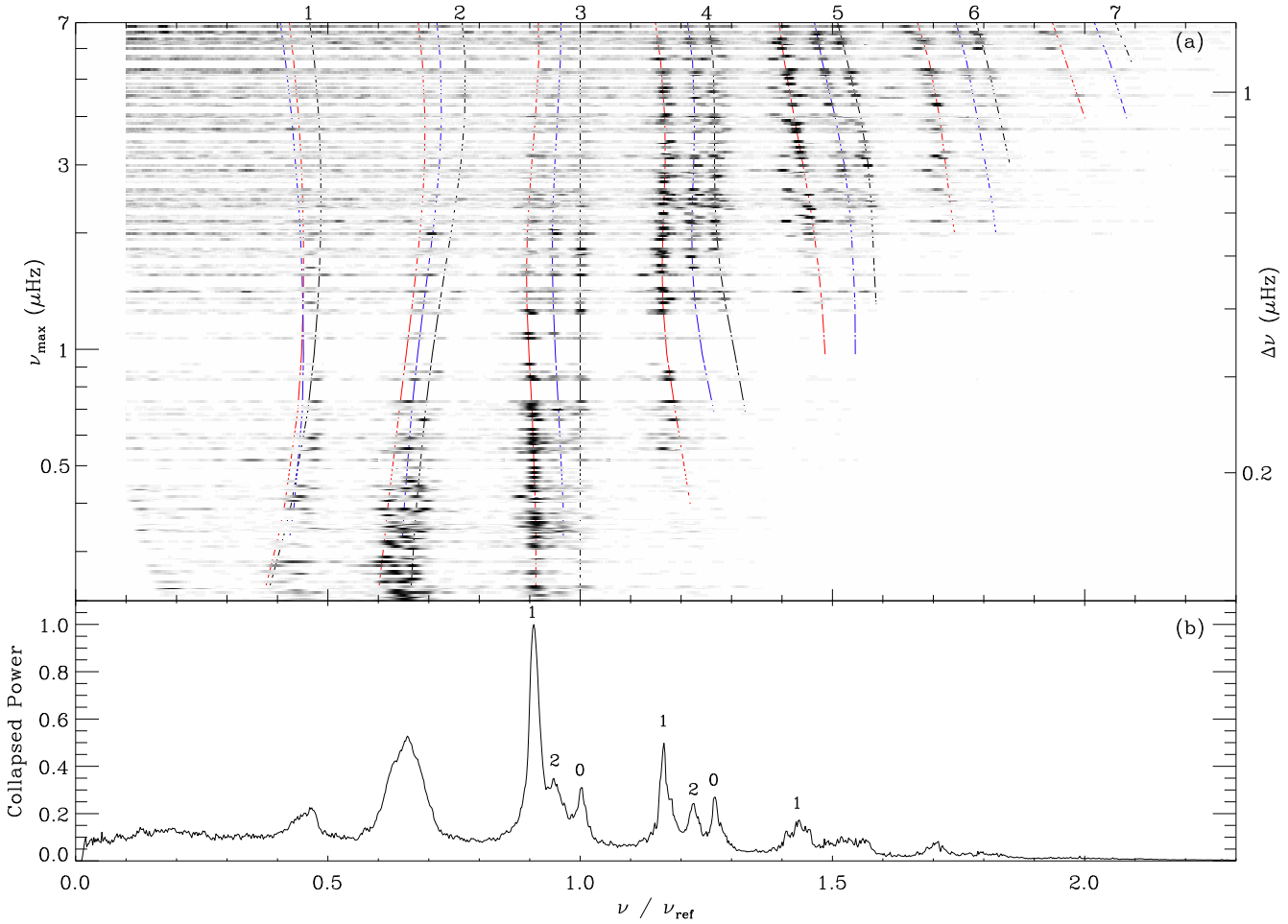

FIG. 3.— (a) Observed power spectra of 195 *Kepler* stars, each displayed as a horizontal band with the level of power indicated by the gray scale. For comparison, ridges of model frequencies are shown in the background for angular degrees $l = 0$ (black), $l = 1$ (red), and $l = 2$ (blue). The radial order is indicated at the top, starting from the fundamental radial mode ($n = 1$). (b) Vertically collapsed version of panel (a) with angular degrees indicated.

that the highly non-asymptotic frequency pattern is dominated by triplets, which is qualitatively different from that of less luminous giants. This explains the fine structure in the Petersen diagram (Soszynski et al. 2004, 2007; Takayama et al. 2013) and, hence, the sub ridges in the period-luminosity diagram suggested by Soszynski et al. (2007).

As a general note of caution the few modes excited and the divergence from asymptotic behavior of the frequencies strongly suggest that using measurements of $\Delta\nu$ and $\nu_{\rm max}$ to estimate stellar masses and radii of luminous giants through the scaling relations could return dubious results.

Whether the non-radial modes 'fade' at some point beyond the red giant branch tip, still remains to be seen. Our observations show that most oscillation power is in the dipole modes and increasing relative to the radial modes towards the more luminous stars. This is evidence that non-radial modes do not fade, but our theoretical models suggest it will be hard to prove because the radial and non-radial modes merge for the two lowest order modes at high luminosities. Without decades-long time series to resolve this, the spectra look like a series of single-degree overtone modes roughly spaced by $\Delta\nu$.

Finally, in our model calculations we found non-radial modes of low inertia (hence visible in Figure 1) whose frequencies are below the fundamental radial mode. We speculate they may be related to the 'f modes' found by Cowling (1941) intermediate between the g and p modes, in the so-called Cowling approximation. This intriguing finding calls for further investigation.

Funding for this Discovery mission is provided by NASA's Science Mission Directorate. We thank the entire Kepler team without whom this investigation would not have been possible. The authors would like to thank Rich Townsend for fruitful discussions and for implementing the 'JCD' variables option in GYRE. Funding for the Stellar Astrophysics Centre is provided by The Danish National Research Foundation (Grant DNRF106). The research is supported by the ASTERISK project (ASTERoseismic Investigations with SONG and Kepler) funded by the European Research Council (Grant agreement no.: 267864). DS acknowledges support from the Australina Research Council. LLK has been supported by the MTA Lendlet-2009 Fellowship, OTKA Grant K83790 and the KTIA URKUT 10-1-2011-0019 grant. SM acknowledges the support by the NASA grant NNX12AE17G and of the European Community's Seventh Framework Pro-

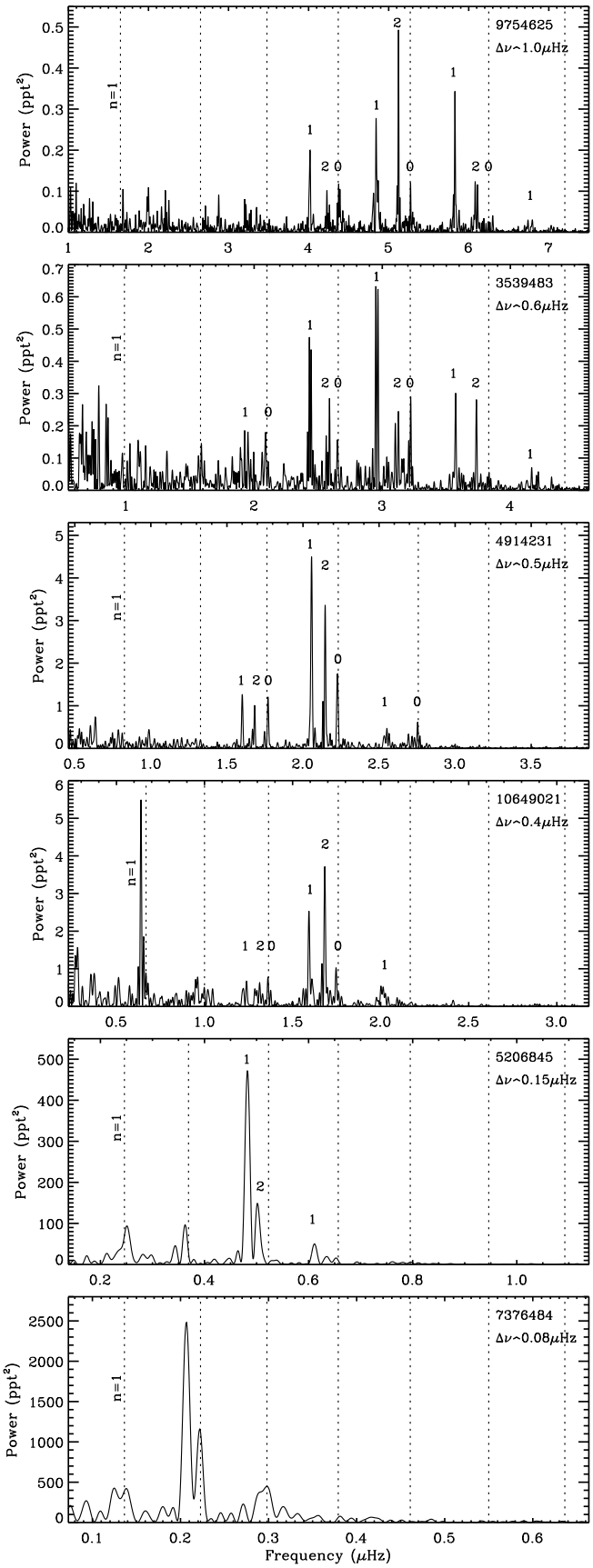

FIG. 4.— Representative power spectra of stars in our sample with $\nu_{\rm max}$ ranging $\sim$ 0.2–5.0μHz. The frequency range has been chosen to roughly align the radial modes indicated by dotted lines for order n =1–7 (n = 1 being the fundamental) from interpolated best-fitting models (see text for details). The KIC-ID, $\Delta\nu$, and the mode degree, l, are shown.

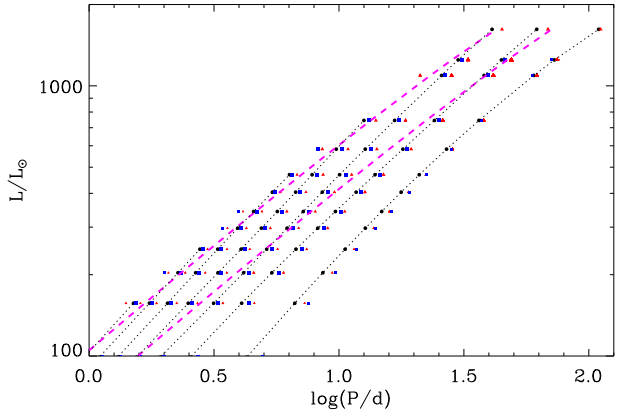

FIG. 5.— Period-Luminosity relation of M giant models of 1M$_\odot$. Notation follows that of Figure 1

gramme (FP7/2007-2013) under grant agreement no. 269194 (IRSES/ASK).

REFERENCES

Aerts, C., Christensen-Dalsgaard, J., Cunha, M., & Kurtz, D. W. 2008, Sol. Phys., 251, 3
Bányai, E., et al. 2013, MNRAS, 436, 1576
Bedding, T. R., Kiss, L. L., Kjeldsen, H., Brewer, B. J., Dind, Z. E., Kawaler, S. D., & Zijlstra, A. A. 2005, MNRAS, 361, 1375
Bedding, T. R., & Zijlstra, A. A. 1998, ApJ, 506, L47
Bedding, T. R., et al. 2010, ApJ, 713, L176
Chaplin, W. J., & Miglio, A. 2013, ARA&A, 51, 353
Christensen-Dalsgaard, J. 2004, Sol. Phys., 220, 137
—. 2008a, Ap&SS, 316, 113
—. 2008b, Ap&SS, 316, 13
Christensen-Dalsgaard, J., Bedding, T. R., & Kjeldsen, H. 1995, ApJ, 443, L29
Christensen-Dalsgaard, J., Kjeldsen, H., & Mattei, J. A. 2001, ApJ, 562, L141
Corsaro, E., et al. 2012, ApJ, 757, 190
Cowling, T. G. 1941, MNRAS, 101, 367
Dupret, M., et al. 2009, A&A, 506, 57
Dziembowski, W. A. 2012, A&A, 539, A83
Dziembowski, W. A., Gough, D. O., Houdek, G., & Sienkiewicz, R. 2001, MNRAS, 328, 601
Dziembowski, W. A., & Soszyński, I. 2010, A&A, 524, A88
Fraser, O. J., Hawley, S. L., Cook, K. H., & Keller, S. C. 2005, AJ, 129, 768
Garcia, R. A., & Stello, D. 2014, in press
Groenewegen, M. A. T. 2004, A&A, 425, 595
Hekker, S. 2013, Advances in Space Research, 52, 1581
Huber, D., et al. 2011, ApJ, 731, 94
Ita, Y., et al. 2004a, MNRAS, 353, 705
—. 2004b, MNRAS, 347, 720
Kiss, L. L., & Bedding, T. R. 2003, MNRAS, 343, L79
Montalbán, J., Miglio, A., Noels, A., Scuflaire, R., & Ventura, P. 2010, ApJ, 721, L182
Mosser, B. 2013, in European Physical Journal Web of Conferences, Vol. 43, European Physical Journal Web of Conferences, 3003
Mosser, B., et al. 2011, A&A, 525, L9
—. 2013, A&A, 559, A137
Olivier, E. A., & Wood, P. R. 2005, MNRAS, 362, 1396
Paxton, B., Bildsten, L., Dotter, A., Herwig, F., Lesaffre, P., & Timmes, F. 2011, ApJS, 192, 3
Paxton, B., et al. 2013, ApJS, 208, 4
Pigulski, A., Pojmański, G., Pilecki, B., & Szczygieł, D. M. 2009, Acta Astron., 59, 33
Riebel, D., Meixner, M., Fraser, O., Srinivasan, S., Cook, K., & Vijh, U. 2010, ApJ, 723, 1195
Soszynski, I., Udalski, A., Kubiak, M., Szymanski, M., Pietrzynski, G., Zebrun, K., Szewczyk, O., & Wyrzykowski, L. 2004, Acta Astron., 54, 129
Soszyński, I., & Wood, P. R. 2013, ApJ, 763, 103
Soszyński, I., Wood, P. R., & Udalski, A. 2013, ApJ, 779, 167
Soszynski, I., et al. 2007, Acta Astron., 57, 201
Spano, M., Mowlavi, N., Eyer, L., Burki, G., Marquette, J.-B., Lecoeur-Taïbi, I., & Tisserand, P. 2011, A&A, 536, A60
Stello, D. 2012, in Astronomical Society of the Pacific Conference Series, Vol. 462, Progress in Solar/Stellar Physics with Helio- and Asteroseismology, ed. H. Shibahashi, M. Takata, & A. E. Lynas-Gray, 200
Tabur, V., Bedding, T. R., Kiss, L. L., Giles, T., Derekas, A., & Moon, T. T. 2010, MNRAS, 409, 777
Takayama, M., Saio, H., & Ita, Y. 2013, MNRAS, 431, 3189
Tassoul, M. 1980, ApJS, 43, 469
Townsend, R. H. D., & Teitler, S. A. 2013, MNRAS, 435, 3406
White, T. R., Bedding, T. R., Stello, D., Christensen-Dalsgaard, J., Huber, D., & Kjeldsen, H. 2011, ApJ, 743, 161
Wood, P. R. 2000, PASA, 17, 18
Wood, P. R., & Sebo, K. M. 1996, MNRAS, 282, 958
Wood, P. R., et al. 1999, in IAU Symposium, Vol. 191, Asymptotic Giant Branch Stars, ed. T. Le Bertre, A. Lebre, & C. Waelkens, 151
Xiong, D.-R., & Deng, L.-C. 2013, Research in Astronomy and Astrophysics, 13, 1269